International Journal of Bifurcation and Chaos, Vol. 15, No. 6 (2005) 2041–2055

QUANTIFYING SMOOTH AND NONSMOOTH REGULAR AND CHAOTIC DYNAMICS

J. AWREJCEWICZ
Technical University of Lodz, Department of Automatics and Biomechanics, 1/15 Stefanowskiego St., 90-924 Lodz, Poland

L. DZYUBAK
Kharkov Polytechnic University, Department of Applied Mathematics, 21 Frunze St., 61002 Kharkov, Ukraine

Received September 10, 2002; Revised June 17, 2003

This paper addresses two main paths of investigations. First, a new numerical method to trace regular and chaotic domains of any nonlinear system governed by ordinary differential equations is proposed. Second, the introduced approach is first testified using the well-known chaotic behavior of a Duffing oscillator and Lorenz system, and is then applied to analysis of discontinuous two-degree-of-freedom self-excited system with friction. Stick-slip and slip-slip chaos is reported, among others.

Keywords: Regular and chaotic dynamics; ordinary differential equations; stick-slip and slip-slip chaos.

1. Introduction

Tracing the research devoted to investigation of chaotic dynamics one may observe that although computations of the Lyapunov exponents are rigorously supported by theory for both smooth [Oseledec, 1968; Wolf *et al.*, 1985] and nonsmooth [Oden & Martins, 1985; Kunze, 2000; Monteiro Marques, 1994; Broglaito, 1999] dynamical systems, many "technical problems" still remain regarding their estimation.

Among others, long time computation is required to trace their limits, and it is in general very difficult to distinguish between slightly exhibited chaotic and quasi-periodic orbits. The mentioned drawbacks increase during analysis of nonsmooth systems. The latter have been observed during analysis of seven-dimensional strongly nonlinear system governing dynamics of the triple pendulum [Awrejcewicz *et al.*, 2002] with impacts, and a special modified approach (see [Awrejcewicz & Olejnik, 2003]) has been proposed to omit the occurred difficulties.

Therefore, our main goal is to propose an alternative approach, for quantifying both regular and chaotic motions, and then to apply it to the analysis of both continuous (Duffing oscillator and Lorenz system) and discontinuous (a mechanical system with friction) systems.

2. Analysis of the Wandering Trajectories

A chaotic behavior of nonlinear deterministic systems supposes a wandering of trajectories of motion around the various equilibrium states. They are characterized by unpredictability and sensitive dependence on the initial conditions. By analyzing trajectories of motion of these systems, it is possible to find the chaotic vibrations regions in control parameters space.

Consider a dynamical system, expressed as the following set of ordinary differential equations

$$\dot{\mathbf{x}} = f(t, \mathbf{x}), \tag{1}$$

where $\mathbf{x} \in R^n$ is the state vector, $f(t, \mathbf{x})$ is defined in $R \times R^n$, and describes the time derivative of the state vector. It is supposed, that $f(t, \mathbf{x})$ is smooth enough to guarantee existence and uniqueness of a solution of the set (1). The right-hand side can be discontinuous while the solution of the set of differential equations (1) remains continuous. For instance, in the cases of discontinuous vector fields of "transversal intersection" and "attracting sliding mode" types a solution to set (1) exists and is unique. The continuous dependence property on the initial conditions $\mathbf{x}^{(0)} = \mathbf{x}(t_0)$ of a solution of set (1) will be used: For every initial condition $\mathbf{x}^{(0)}$, $\tilde{\mathbf{x}}^{(0)} \in R^n$, for every number $T > 0$, no matter how large, and for every preassigned arbitrary small $\varepsilon > 0$ it is possible to indicate a positive number $\delta > 0$ such that if the distance ρ between $\mathbf{x}^{(0)}$ and $\tilde{\mathbf{x}}^{(0)}$, $\rho(\mathbf{x}^{(0)}, \tilde{\mathbf{x}}^{(0)}) < \delta$, and $|t| \leq T$, the following inequality is satisfied

$$\rho(\mathbf{x}(t), \tilde{\mathbf{x}}(t)) < \varepsilon.$$

That is if the initial points are chosen close enough, than during the preassigned arbitrary large time interval $-T \leq t \leq T$ the distance between simultaneous positions of moving points will be less, given positive number ε.

A metric ρ on R^n can be determined in various ways, for example $\rho_1(\mathbf{x}, \tilde{\mathbf{x}}) = \sqrt{\sum_{i=1}^{n}(x_i - \tilde{x}_i)^2}$, $\rho_2(\mathbf{x}, \tilde{\mathbf{x}}) = \sum_{i=1}^{n}|x_i - \tilde{x}_i|$ or $\rho_3(\mathbf{x}, \tilde{\mathbf{x}}) = \max_{1\leq i\leq n}|x_i - \tilde{x}_i|$, where $\mathbf{x} = (x_1, x_2, \ldots, x_n) \in R^n$, $\tilde{\mathbf{x}} = (\tilde{x}_1, \tilde{x}_2, \ldots, \tilde{x}_n) \in R^n$.

Being interested in tracing chaotic and regular dynamics, we shall suppose that with the increase of time all trajectories with remain in the closed bounded domain of a phase space, i.e.

$$\exists C_i \in R : \max_t |x_i(t)| \leq C_i \quad (i = 1, 2, \ldots, n).$$

To analyze trajectories of the set (1), we introduce the characteristic vibration amplitudes A_i of components of the motion $x_i(t)$ $(i = 1, 2, \ldots, n)$:

$$A_i = \frac{1}{2}\left|\max_{t_1\leq t\leq T} x_i(t) - \min_{t_1\leq t\leq T} x_i(t)\right| \quad (i = 1, 2, \ldots, n).$$

Here $[t_1, T] \subset [t_0, T]$ and $[t_0, T]$ is the time interval, in which the trajectory is considered. The interval $[t_0, t_1]$ is the time interval, in which all transient processes are damped. The characteristic vibration amplitudes A_i can be calculated simultaneously to the integration of the trajectory.

For the sake of our investigations it seems the most convenient to use the embedding theorem and to consider an n-dimensional parallelepiped instead of a hyper-sphere with the center at point $\mathbf{x}$. Recall the embedding theorem:

If $S_\varepsilon(\mathbf{x}) = \{\tilde{\mathbf{x}} \in R^n : \rho(\mathbf{x}, \tilde{\mathbf{x}}) < \varepsilon\}$ is the hyper-sphere with center at the point $\mathbf{x}$ and with radius ε and $P_{\varepsilon_1,\varepsilon_2,\ldots,\varepsilon_n}(\mathbf{x}) = \{\tilde{\mathbf{x}} \in R^n : |x_i - \tilde{x}_i| < \varepsilon_i\}$ is the n-dimensional parallelepiped then for any $\varepsilon > 0$ there is parallelepiped $P_{\varepsilon_1,\varepsilon_2,\ldots,\varepsilon_n}(\mathbf{x})$ such that $P_{\varepsilon_1,\varepsilon_2,\ldots,\varepsilon_n}(\mathbf{x}) \subset S_\varepsilon(\mathbf{x})$. And conversely, for any parallelepiped $P_{\varepsilon_1,\varepsilon_2,\ldots,\varepsilon_n}(\mathbf{x})$ it is possible to indicate $\varepsilon > 0$ such that $S_\varepsilon(\mathbf{x}) \subset P_{\varepsilon_1,\varepsilon_2,\ldots,\varepsilon_n}(\mathbf{x})$.

Let us choose in the parallelepiped $P_{\delta_1,\delta_2,\ldots,\delta_n}(\mathbf{x}^{(0)})$ two neighboring initial points $\mathbf{x}^{(0)}$ and $\tilde{\mathbf{x}}^{(0)}$ such that $|x_i^{(0)} - \tilde{x}_i^{(0)}| < \delta_i$, where δ_i is small in comparison with A_i $(i = 1, 2, \ldots, n)$. In the case of regular motion it is expected that the ε_i used in inequality $|x_i(t) - \tilde{x}_i(t)| < \varepsilon_i$ is also small in comparison with A_i, for $i = 1, 2, \ldots, n$. The wandering orbits attempt to fill up some bounded domain of the phase space. At instant t_0 the neighboring trajectories diverge exponentially. Hence, for some instant t_1 the absolute values of differences $|x_i(t) - \tilde{x}_i(t)|$ can take any values in closed interval $[0, 2A_i]$. If the differences $|x_i(t) - \tilde{x}_i(t)|$ are equal to zero for some instants $\{t_k^*\}$, $(t_k^* \in [t_1, T])$, then the trajectories $\mathbf{x}(t)$ and $\tilde{\mathbf{x}}(t)$ either are intersecting or have points of contact at these instants. Obviously, $2A_i$ are the maximal values for these differences, and for some time instants this value is permissible. Let us introduce an auxiliary parameter $\alpha, 0 < \alpha < 1$ and let αA_i be referred to as divergence measures of observable trajectories in the directions of generalized coordinates x_i $(i = 1, 2, \ldots, n)$. By analyzing Eq. (1) and its equilibrium states it is easy to choose parameter $\alpha, 0 < \alpha < 1$, such that if the following statement is satisfied,

$$\exists t^* \in [t_1, T] : |x_i(t^*) - \tilde{x}_i(t^*)| > \alpha A_i, \quad (i = 1, 2, \ldots, n). \tag{2}$$

It follows that there is a time interval or a set of time intervals, for which the affixes of the trajectories $\mathbf{x}(t)$ and $\tilde{\mathbf{x}}(t)$, closed at the initial instant, move around various equilibrium states or these trajectories are sensitive to changing of the initial conditions. Thus, these trajectories are the wandering ones. Indeed, as it has already been mentioned, all trajectories are in the closed bounded domain in R^n. With the aid of parameter α the divergence measures of the trajectories αA_i have been chosen, which is *inadmissible* for the case of "regularity" of the motion. Note that this choice is nonunique and the parameter α can take various values in interval $(0, 1)$. It is clear, however, that if α is close to 0 and $|x_i(t) - \tilde{x}_i(t)| < \alpha A_i$ when $t \in [t_0, T]$, then the trajectories do not diverge and the trajectories are regular. There are values of the parameter α, which *a priori* correspond to inadmissible divergence measures αA_i $(i = 1, 2, \ldots, n)$ of the trajectories in the sense of "regularity". For example, $\alpha \in \{1/3, 1/2, 2/3, 3/4\}$ or other choices are possible. If the representative points of the observable trajectories move chaotically, then for another choice α from the set of *a priori* "appropriate" α, the divergence of the trajectories will be recorded at another time instant t^*. As numerical experiments show, the obtained domains of chaotic behavior with various *a priori* "appropriate" values of α are practically congruent. Therefore, in this work figures for different values of α are not presented.

A similar nonunique choice of parameters occurs when applying other criteria for the chaotic oscillations. For instance, consider the procedure for calculating the Lyapunov exponents $d(t) = d_0 2^{\lambda t}$. Here λ is the Lyapunov exponent, d_0 the initial distance measure between the starting points and $d(t)$ the distance between trajectories in instant t. The base 2 is chosen for simplicity. In all other respects, the parameter $\alpha > 1$ in the relation $d(t) = d_0 \alpha^{\lambda t}$ is arbitrary. That is, the parameter α can take different values, for example, $\alpha \in \{2, 3, 4, 5\}$ or other choices are possible. In general, the specificity of numerical approaches requires that all parameters have to be fixed.

It can be commented that this paper's approach and well-known Wolf's algorithm of determining the Lyapunov exponents are both realized by computer simulation. According to Wolf's algorithm, the calculation of the Lyapunov exponent λ as the measure of the trajectory divergence begins with the choosing of a basic trajectory $\mathbf{x}^*(t, \mathbf{x}^{(0)})$. At each time step t_k the dynamical system (1) is integrated again with any neighboring points $\mathbf{x}^*(t_k) + \eta$ acting as the initial conditions. Thus, to find λ the governing equations (1) and the corresponding variational equations $\dot{\eta} = \mathbf{A} \cdot \eta$, in which $\mathbf{A}$ is matrix of partial derivatives $\nabla f(\mathbf{x}^*(t_k))$, are solved N times (where N is the number of the time steps). Averaging over a long time results in a reliable value of λ variations of distances between the trajectories. To realize this paper's approach it is enough to solve the equations governing the dynamical system only two times for each selected trajectory.

The α parameter might have another physical interpretation. Assume that for the nonlinear dynamical system under investigation, it is possible to identify the singular points (equilibria). In the case, for instance, of two-well potential systems we have two nodes and one saddle. An external periodic excitation applied to such one-degree-of-freedom system may cause a chaotic response. Chaos is characterized by the unpredictable switches between the two potential wells. A phase point may wander between all three singular points. Consider two neighboring nodes. As a result of switching neighbors at the initial instant, representative points of the phase trajectories are in motion about various equilibrium states afterward. Hence a choice of α, on the relation $\alpha A_i \cong (1/2)d$, is related to the distance d between the two nodes separated by a saddle. However, many of nonlinear dynamical systems do not have analytical solutions, and sometimes it is laborious to find the singular points. This situation occurs often in nonsmooth dynamical systems. In this case it is recommended to take the α parameter from *a priori* "appropriate" values.

Our approach has been successfully applied to the case of smooth and nonsmooth systems. By varying parameters and using condition (2), it is possible to find domains of chaotic motion (including transient and alternating chaos) and domains of regular motion.

Remark. All inequalities (2) do not have to be checked for the case, when the equations of motion under investigation can be transformed to normal form. It means that the inequalities related to velocities $x_j = \dot{x}_i$ may be canceled. In other words, solutions related to regular motion with respect to x_i are also regular in relation to $x_j = \dot{x}_i$, where $i, j \in \{\overline{1, n}\}$.

3. Chaos in the "Smooth" Duffing Equation and the Lorenz System

Let us consider the nonautonomous Duffing equation:

$$\ddot{x} + \gamma\dot{x} - \frac{1}{2}x(1 - x^2) = f\cos\omega t. \tag{3}$$

For this system $A_x = (1/2)|\max_{t_1 \le t \le T} x(t) - \min_{t_1 \le t \le T} x(t)|$ and the condition (2) has the form:

$$\exists t^* \in [t_1, T] : |x(t^*) - \tilde{x}(t^*)| > \alpha A_x.$$

Using this condition, different planes of parameters of Duffing equation have been investigated.

The dynamics of this equation is determined by three parameters f, ω, γ and the initial conditions $x(0)$ and $\dot{x}(0)$. In Fig. 1(a), dots represent the domains of chaotic behavior in the amplitude — frequency of excitation (ω, f) plane for fixed value of parameter $\gamma = 0.15$ and initial conditions $x(0) = 0.1$, $\dot{x}(0) = 0.01$. The time period for the simulation is $100\pi/\omega$ nondimensional time units. During computations, one half of the time period corresponds to the time interval $[t_0, t_1]$, where transient processes are damped. The integration step size is $\pi/30\omega$. The space of parameters has been uniformly sampled in the rectangular $(0 < \omega \leq 1.15;\ 0 < f \leq 0.55)$ by 40×40 nodal points. Initial conditions of the closed trajectories are distinguished by 0.5% with ratio to characteristic vibration amplitudes A_i, e.g. the starting points of these trajectories are in the two-dimensional parallelepiped $(|x(t_0) - \tilde{x}(t_0)| < 0.005A_x,\ |\dot{x}(t_0) - \tilde{\dot{x}}(t_0)| < 0.005A_{\dot{x}})$. The parameter α is chosen equal to 1/3.

The obtained domains agree well with the smooth threshold, that is, corresponding to the homoclinic trajectory criterion [Holmes, 1979]. The domains are remarkably conforming to the results of the investigations based on the calculation of the Lyapunov exponents, which was carried out with Wolf's algorithm [Moon, 1987; Wolf *et al.*, 1985].

In Fig. 1(b) the chaotic domains for the equation $\ddot{x} + \gamma\dot{x} - x(1 - x^2) = f\cos\omega t$ are depicted in the amplitude — damping coefficient plane (γ, f), for fixed frequency $\omega = 1.7$, and initial conditions $x(0) = 0.1$, $\dot{x}(0) = 0.01$. The time period for the simulation is $100\pi/\omega$ nondimensional time units. We have decided that the half of time period corresponds to the time interval $[t_0, t_1]$ in the space of which all transient processes are damped. The integration step size is $\pi/20\omega$. The space of parameters is uniformly sampled in the rectangular $(0 < \gamma \leq 1.35;\ 0 < f \leq 2.15)$ by 40×40 nodal points. As in the previous case, the initial conditions of the closed trajectories are distinguished by 0.5% with ratio to characteristic vibration amplitudes A_i, and the parameter α is set equal to 1/3.

The computed domains agree with the smooth threshold corresponding to the homoclinic trajectory criterion [Holmes, 1979],

$$f > \frac{4}{3}\gamma\frac{\mathrm{ch}(\pi\omega/2)}{\sqrt{2}\pi\omega}.$$

(In a case of Eq. (3) a change of variables has been introduced.) The real boundary of chaotic oscillations in the plane (γ, f) is not linear and qualitatively corresponds to that found by our numerical method. In both cases (a) and (b) the chaotic domains are multiply connected.

Phase planes of the initial conditions have been analyzed for Eq. (3) for fixed values of parameters $\gamma = 0.15$, $\omega = 0.8$. Figure 2 shows the phase planes of the initial conditions for different values of the amplitude of excitation: (a) $f = 0.06$ and

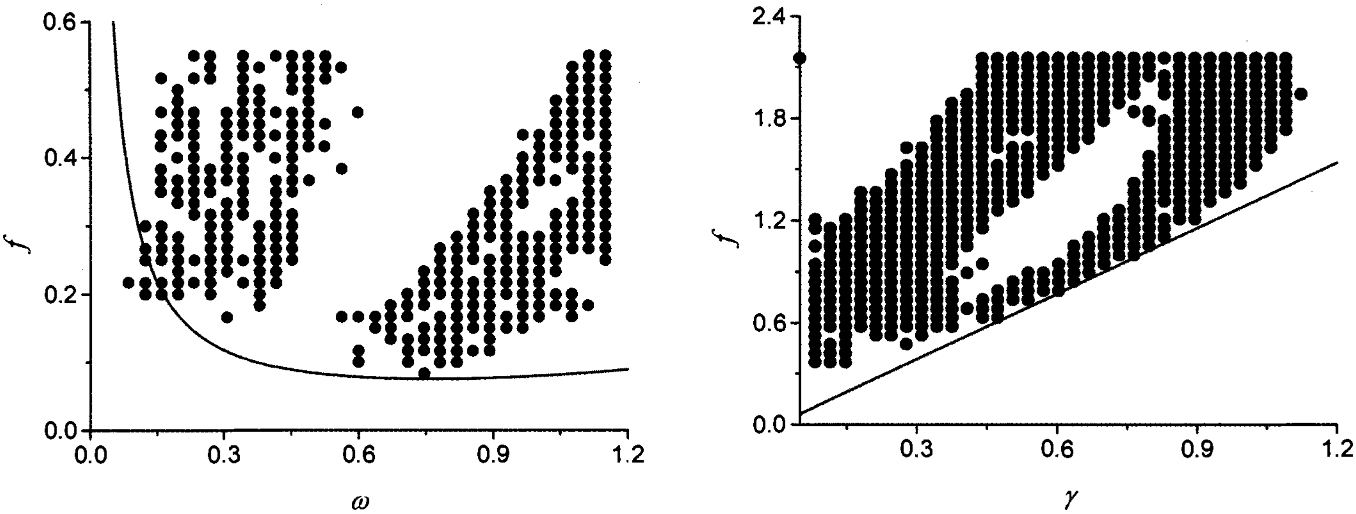

(a) (b)

Fig. 1. Domains of chaotic behavior for the Duffing equation: (a) in the (ω, f) plane ($\gamma = 0.15$, $x(0) = 0.1$, $\dot{x}(0) = 0.01$); (b) in the (γ, f) plane ($\omega = 1.7$, $x(0) = 0.1$, $\dot{x}(0) = 0.01$). The smooth threshold corresponds to the homoclinic trajectory criterion.

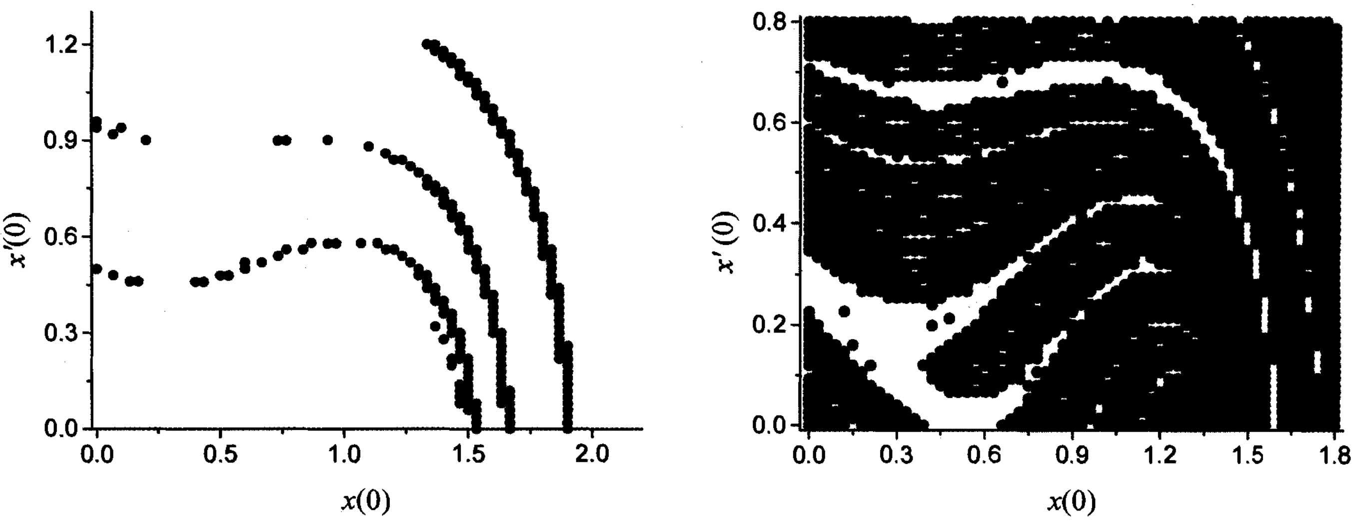

Fig. 2. The initial conditions phase plane for the Duffing equation for different values of the amplitude of excitation ($\gamma = 0.15$, $\omega = 0.8$): (a) $f = 0.06$; (b) $f = 0.1$.

(b) $f = 0.1$. Depending on the initial conditions both chaotic and regular motion may appear. The instability peculiar to chaotic vibrations is observed close to the separatrix branches. While increasing the f value the domains of chaotic vibrations are fast augmenting. The time period for the simulation has been taken as $100\pi/\omega$ nondimensional time units, and the integration step size is equal to $\pi/20\omega$. The space of parameters is uniformly sampled in the rectangular ($0 < x(0) \leq 1.8$; $0 < \dot{x}(0) \leq 0.8$) by 40×40 nodal points. Initial conditions of the closed trajectories are distinguished by 0.5% with a ratio to characteristic vibration amplitudes A_i (the parameter α has set equal to 1/3).

Now we consider the Lorenz system, of the form

$$\begin{cases} \dot{x} = \sigma(y - x), \\ \dot{y} = \rho x - y - xz, \\ \dot{z} = xy - \beta z \end{cases} \tag{4}$$

Using the conditions (2), which for the system (4) has the form

$$\exists t^* \in [t_1, T] :$$
$$\{(|x(t^*) - \tilde{x}(t^*)| > \alpha A_x) \vee (|y(t^*) - \tilde{y}(t^*)| > \alpha A_y) \vee (|z(t^*) - \tilde{z}(t^*)| > \alpha A_z)\},$$

$$A_x = \frac{1}{2}\left|\max_{t_1 \leq t \leq T} x(t) - \min_{t_1 \leq t \leq T} x(t)\right|,$$

$$A_y = \frac{1}{2}\left|\max_{t_1 \leq t \leq T} y(t) - \min_{t_1 \leq t \leq T} y(t)\right|,$$

$$A_z = \frac{1}{2}\left|\max_{t_1 \leq t \leq T} z(t) - \min_{t_1 \leq t \leq T} z(t)\right|,$$

the different planes of parameters of the Lorenz system are investigated.

In Fig. 3, the phase space of the initial conditions for the Lorenz system is presented at fixed values of parameters $\sigma = 10$, $\beta = 8/3$, $\rho = 16$. The time period for the simulation is 90 nondimensional time units. We decided that 2/3 of the time period should be equal to the time interval $[t_0, t_1]$, during which all transient processes are damped. The integration step size is 0.03

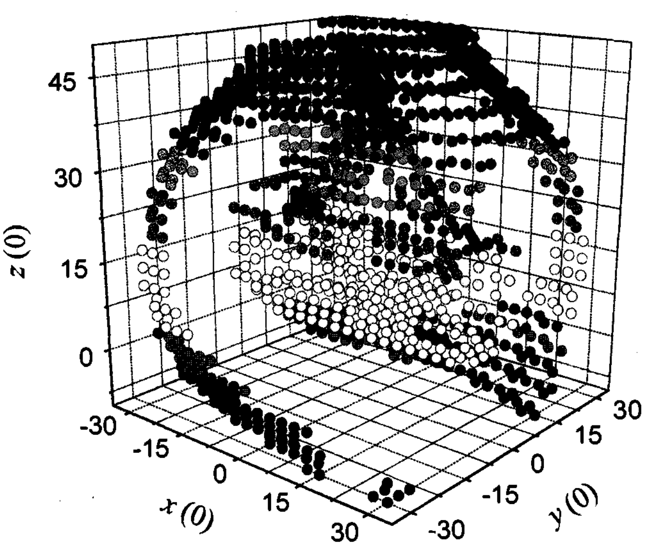

Fig. 3. The phase space of the initial conditions for the Lorenz system ($\sigma = 10$, $\beta = 8/3$, $\rho = 16$).

nondimensional time units. The space of parameters is uniformly sampled in the rectangular parallelepiped ($-30 < x(0) \leq 30$; $-30 < y(0) \leq 30 - 10 < z(0) \leq 50$) by $20 \times 20 \times 20$ nodal points. Initial conditions of the closed trajectories are distinguished by 0.5% of the characteristic vibration amplitudes A_x, A_y, A_z, *e.g.* the starting points of these trajectories are in the three-dimensional parallelepiped ($|x(t_0) - \tilde{x}(t_0)| < 0.005A_x$, $|y(t_0) - \tilde{y}(t_0)| < 0.005A_y$, $|z(t_0) - \tilde{z}(t_0)| < 0.005A_z$). The parameter α is set equal to 1/3.

As in the case of the Duffing equation, the instability peculiar to chaotic vibrations is observed close to the separatrix branches and by increasing ρ the domains of chaotic vibrations expand fast.

In Fig. 4, the domain of chaotic vibrations in the (β, ρ) parameter plane is shown for fixed $\sigma = 10$, $x(0) = 5$, $y(0) = 5$, $z(0) = 10$. The time period for the simulation is 90 nondimensional time units. We have chosen as 2/3 of the time period to be the time interval $[t_0, t_1]$, during which all transient processes are damped. The integration step size is 0.03 nondimensional time units. The space of parameters is uniformly sampled in the rectangular ($0 < \beta \leq 15$; $0 < \rho \leq 50$) by 30×30 nodal points. Initial conditions of the closed trajectories are distinguished by 0.5% of the characteristic vibration amplitudes A_x, A_y, A_z. The α parameter is set equal to 1/3. These results conform well with the investigations and diagrams presented in [Moon, 1987].

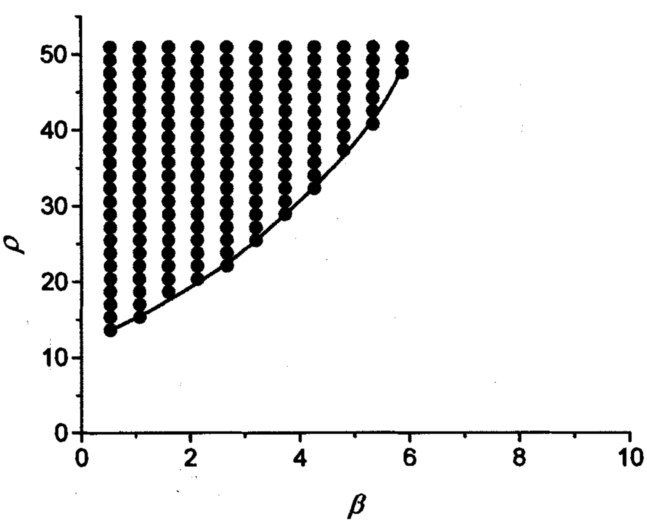

Fig. 4. The domain of chaotic vibrations for the Lorenz equations in the (β, ρ) plane ($\sigma = 10$, $x(0) = 5$, $y(0) = 5$, $z(0) = 10$).

4. Discontinuous Autonomous Two-Degree-of-Freedom System with Dry and Viscous Friction

4.1. *The model*

Consider two masses m_1 and m_2 (as shown in Fig. 5) which are moving on a driving belt. The belt is moving at a constant velocity v_0. The mass m_1 is attached to inertial space by a spring k_1. Masses m_1 and m_2 are coupled by a spring k_2. A friction force T_i acts between the mass m_i and belt which depends on the relative velocity w_i ($i = 1, 2$). These two-degree-of-freedom autonomous oscillations are governed by the following second-order set of differential equations

$$\begin{cases} m_1\ddot{x}_1 = -k_1x_1 - k_2x_1 + k_2x_2 + T_1(w_1) \\ m_2\ddot{x}_2 = -k_2x_2 + k_2x_1 + T_2(w_2), \end{cases} \tag{5}$$

where

$$w_i = v_0 - \dot{x}_i, \quad (i = 1, 2).$$

We will consider the following friction model (see Fig. 6):

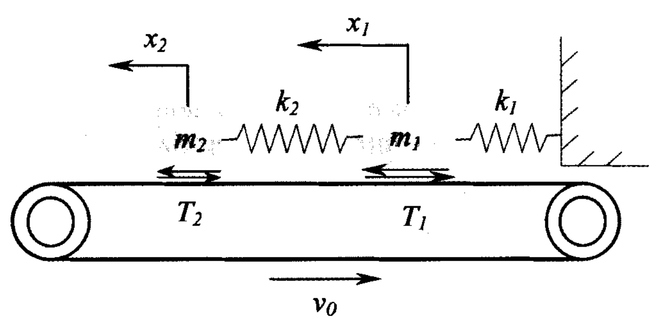

Fig. 5. Analyzed 2-DOF model with friction.

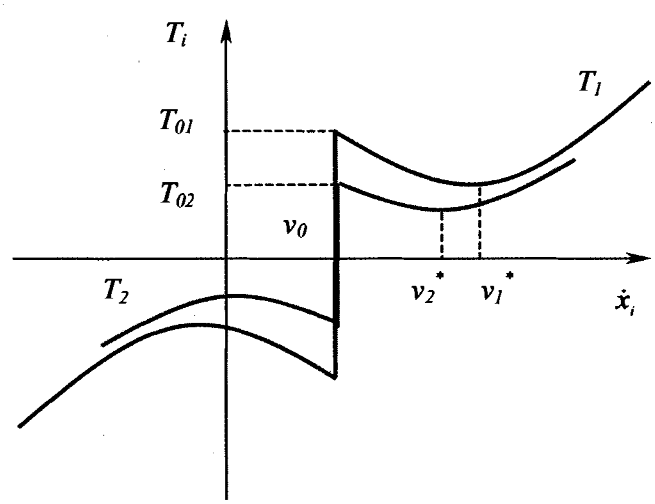

Fig. 6. Dry and viscous friction model.

$$T_i(w_i) = T_{0i} \operatorname{sign} w_i - \alpha_i(T_{0i})w_i + \beta_i(T_{0i})w_i^3,$$
$$\alpha_i = \frac{3}{4}\frac{T_{0i}}{v_i^*}, \quad \beta_i = \frac{T_{0i}}{4(v_i^*)^3} \qquad (i = 1, 2).$$

Here the maximum static friction force is denoted by T_{0i} and v_i^* is the velocity which corresponds to the local extremum value of $T_i(w_i)$ $(i = 1, 2)$.

4.2. *A stick-slip and slip-slip motion*

Let us find the stick-slip and slip-slip domains of the chaotic or regular motion. If the solution $\mathbf{x}(t)$ of the set (5) is known, it is easy to obtain the set of time intervals $\{\Delta t_{st\ i}\}$ during which the following condition holds

$$\dot{x}_i = v_0, \quad (i = 1, 2). \tag{6}$$

This corresponds to the presence of "stick" in the vibrations of *i*st oscillator. The maximum time interval $\max \Delta t_{st\,i}$ from the set $\{\Delta t_{st\,i}\}$ can be considered as the characteristic of the specific motion.

Let a space of parameters under investigation have the velocity of the belt v_0 as a coordinate. The dynamics of the oscillators will increase with magnification of v_0. Hence, even a very small value of $\max \Delta t_{st\,i}$ will indicate a presence of a "stick" during vibrations. In this case, under an appropriate choice of the auxiliary parameter $0 < \delta < 1$, a check of the following control condition

$$v_0 \max \Delta t_{st\,i} < \delta A_i \quad (i = 1, 2) \tag{7}$$

allows one to trace the presence of a "stick" motion. The constant δ defines the smallness of the "stick"-segments on the phase plane in comparison with the characteristic vibration amplitudes A_i of the components of motion $x_i(t)$ $(i = 1, 2)$. Thus, if condition (7) holds, then the i-oscillator is in the slip-slip motion, and the other one is in the stick-slip motion.

4.3. *Chaotic and regular stick-slip and slip-slip oscillations*

Note that conditions (2) for the system (5) can be presented in the following form

$$\exists t^* \in [t_1, T]:$$
$$\{(|x_1(t^*) - \tilde{x}_1(t^*)| > \alpha A_1) \vee (|x_2(t^*) - \tilde{x}_2(t^*)| > \alpha A_2)\}$$
$$\Downarrow \qquad\qquad\qquad \Downarrow$$

chaos of the first oscillator   chaos of the second oscillator

In addition, the conditions (6), (7) of the space of parameters (v_0, T_{01}, T_{02}) for the system (5) have been investigated after a coordinate sampling. The domains, where chaotic behaviors of the first and second oscillators are possible, were found, including stick-slip and slip-slip motion. All numerical calculations are carried out for the following fixed values (all of the parameters are considered in the system "SI"): $m_1 = 4$, $m_2 = 3$, $k_1 = 11.77$, $k_2 = 7.85$, $v_1^* = 4$, $v_2^* = 3$.

The following initial conditions are taken: $x_1(0) = 0.01$, $\dot{x}_1(0) = 0.5$, $x_2(0) = 0.01$, $\dot{x}_2(0) = 0.5$. The time period for the simulation is 120 time units. During computations, a half of time period corresponds to the time interval $[t_0, t_1]$, where transitional processes are damped. The integration step size is chosen equal to 2.5×10^{-3} time units. The space of parameters is uniformly sampled in the rectangular parallelepiped $(0 < v_0 \leq 4;\ 0 < T_{01} \leq 50,\ 0 < T_{02} \leq 50)$ by $40 \times 50 \times 50$ nodal points. Initial conditions of the closed trajectories are distinguished by 0.5% with ratio to characteristic vibration amplitudes A_i $(i = 1, 2)$, e.g. the starting points of these trajectories are in the four-dimensional parallelepiped $|x_i(t_0) - \tilde{x}_i(t_0)| < 0.005 A_i$, $i = \overline{1, 4}$. The parameter α is set equal to 1/3.

Figure 7 in a section $T_{02} = 19.62$ of the parameters space (v_0, T_{01}, T_{02}) displays the domains, where chaotic vibrations of the (a) first and (b) second oscillators are possible. It is interesting, that these regions are almost congruent. In other words, during numerical simulation we do not encounter the situation when only one of the oscillators moves chaotically. It is remarkable also, that there appear chaotic "islets" in domains of periodic motion. In a section $T_{01} = 29.43$ (see Fig. 8) the chaotic vibrations domains of (a) first and (b) second oscillators are also almost practically congruent.

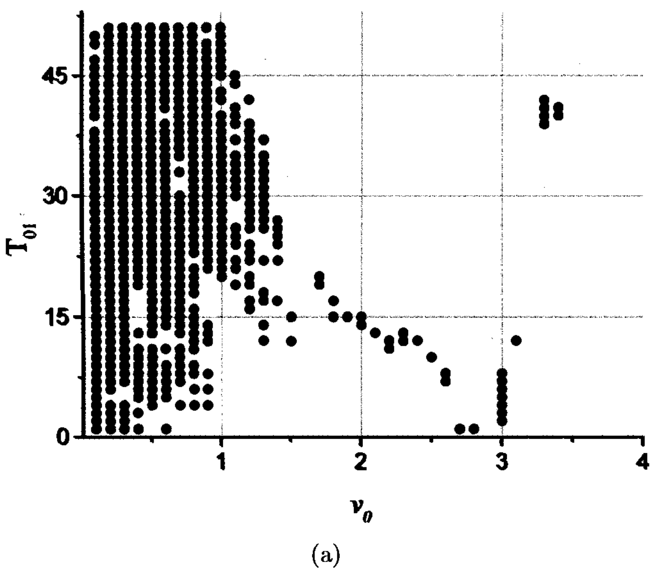

Fig. 7. Domains of chaotic vibrations of the (a) first and (b) second oscillators in the (v_0, T_{01}) plane ($T_{02} = 19.62$, $x_1(0) = 0.01$, $\dot{x}_1(0) = 0.5$, $x_2(0) = 0.01$, $\dot{x}_2(0) = 0.5$).

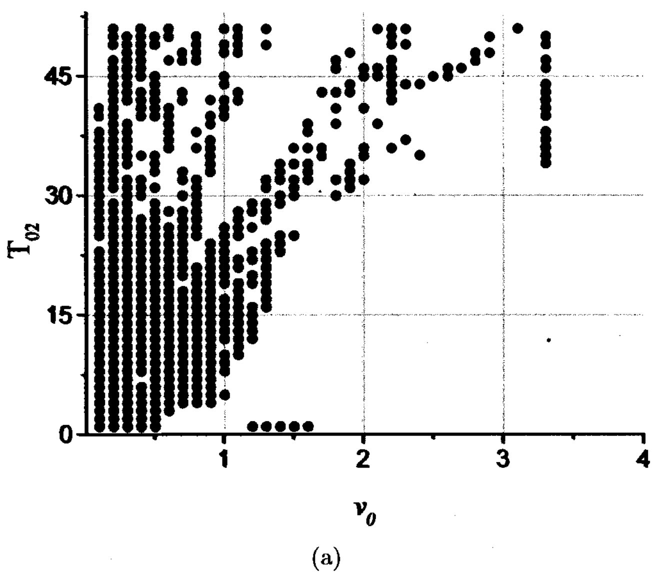

Fig. 8. Domains of chaotic vibrations of the (a) first and (b) second oscillators in the (v_0, T_{02}) plane ($T_{01} = 29.43$, $x_1(0) = 0.01$, $\dot{x}_1(0) = 0.5$, $x_2(0) = 0.01$, $\dot{x}_2(0) = 0.5$).

In Figs. 9 and 10 the domains of stick-slip oscillations are shown, which correspond to $\Delta t_{st\,i}$ various "adhesion" time of the oscillators to the belt [when $5 < \max \Delta t_{st\,i}$, $2 < \max \Delta t_{st\,i} < 5$, $0.5 < \max \Delta t_{st\,i} < 2$, $\max \Delta t_{st\,i} < 0.5$ $(i = 1, 2)$]. The mentioned domains are reported in a section $T_{02} = 19.62$ (see Fig. 9) of the parameters space (v_0, T_{01}, T_{02}) for the (a) first and (b) second oscillators and also in a section $T_{01} = 29.43$ (see Fig. 10) for the (a) first and (b) second oscillators. Both in Figs. 9 and 10 blue dots represent the domains, where the maximum time interval $\max \Delta t_{st\ i} < 0.5$ and the inequality (7) is not satisfied [$i = 1$ for cases (a), $i = 2$ for cases (b)]. Though the maximum time interval of "adhesion" is too little, one observes that owing to the dynamical process, the segment on a phase plane corresponding to "adhesion" of an oscillator is more than δ of the characteristic vibration

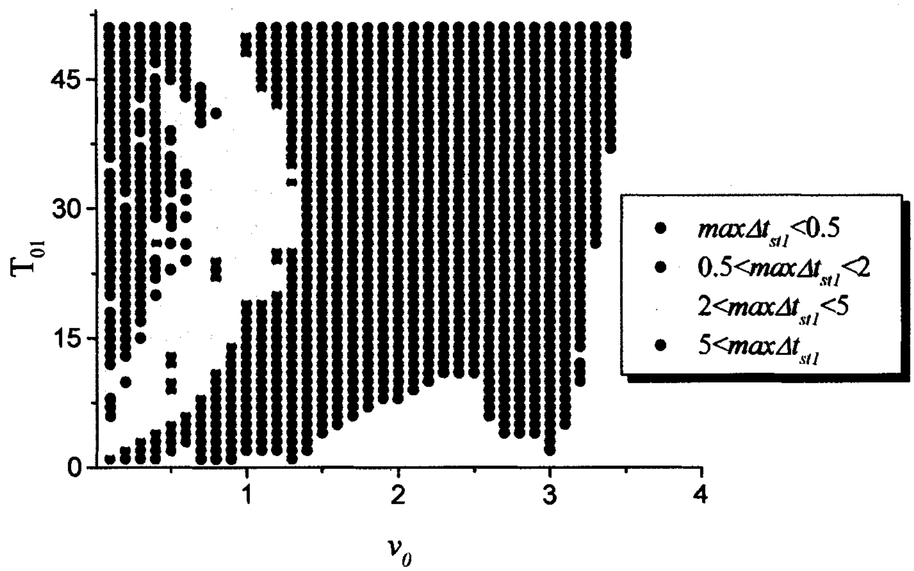

(a)

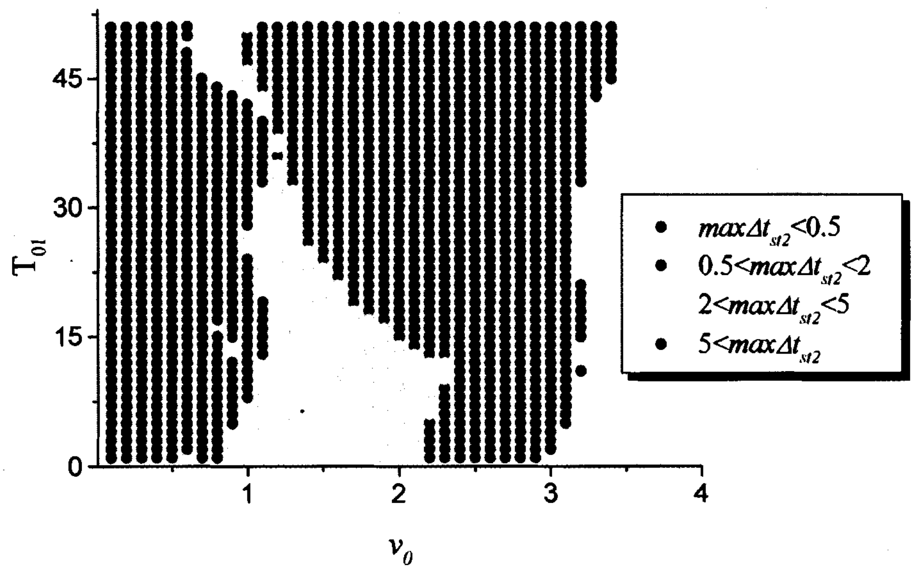

(b)

Fig. 9. Domains of stick-slip oscillations of the (a) first and (b) second oscillators in the (v_0, T_{01}) plane ($T_{02} = 19.62$, $x_1(0) = 0.01$, $\dot{x}_1(0) = 0.5$, $x_2(0) = 0.01$, $\dot{x}_2(0) = 0.5$) with various "adhesion" times of the oscillators to the belt.

amplitude A_i. In the present investigations, it has been taken $\delta = 0.1$.

Figure 11 shows the trajectories of the first and second oscillators on a phase plane corresponding to the domain of the chaotic vibrations [see Figs. 7(a) and 7(b)]. Stick refers to $2 < \max \Delta t_{sti} < 5$ for the first oscillator and to $5 < \max \Delta t_{sti}$ for the second oscillator, [see Figs. 9(a) and 9(b)]. The phase portraits plotted in Fig. 12 correspond to chaotic behavior domains observed in Figs. 8(a) and 8(b).

Figures 13 and 14 display periodic vibrations of both oscillators. In Fig. 14, the first oscillator moves without a stick condition. All these data demonstrate a very good agreement with the obtained chaotic and regular vibration domains (see Fig. 7) and with the domains of stick-slip and slip-slip motion (see Fig. 9).

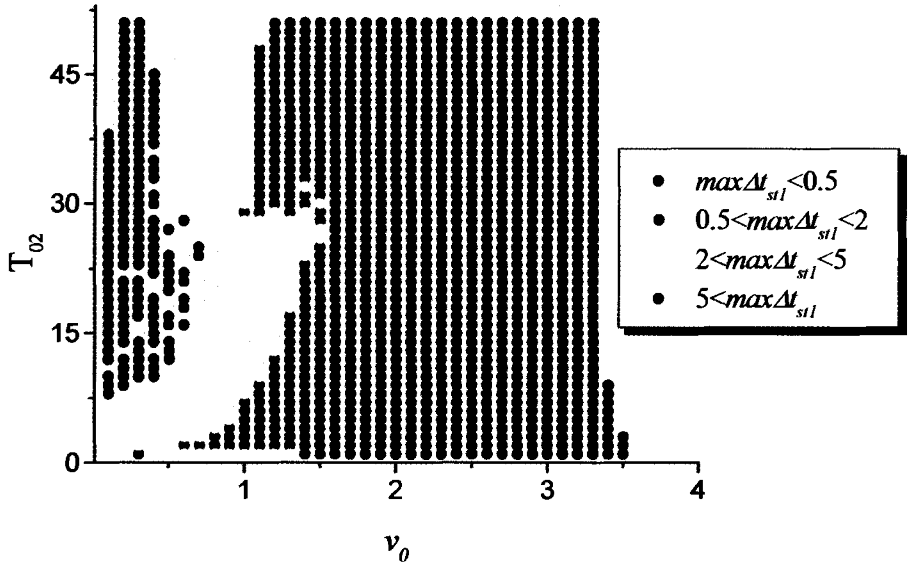

(a)

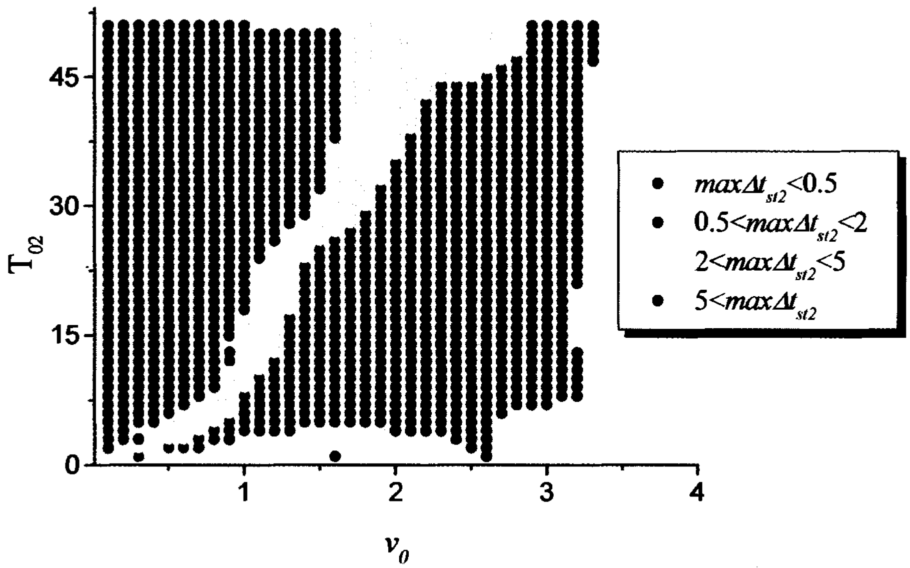

(b)

Fig. 10. Domains of stick-slip oscillations of the (a) first and (b) second oscillators in the (v_0, T_{02}) plane ($T_{01} = 29.43$, $x_1(0) = 0.01$, $\dot{x}_1(0) = 0.5$, $x_2(0) = 0.01$, $\dot{x}_2(0) = 0.5$) with various "adhesion" times of the oscillators to the belt.

In Figs. 15(a)–15(c) one may observe the origin of chaos with a passage (see also Fig. 8) from the stability domain [Fig. 15(a)] to the instability domain [Figs. 15(b) and 15(c)]. In the first case a regular motion around all three states is displayed. Then the first oscillator moves around various states with unpredictable jumping between states.

The comparison of Figs. 7 and 9 and also of Figs. 8 and 10 testifies that our system mainly exhibits stick-slip chaos. Slip-slip chaotic motion is possible in the small domain of neighborhood of $v_0 = 3.3-3.4$ only for the second oscillator. The corresponding examples are shown in Figs. 16 and 17.

The coupled oscillators with friction have many aspects to investigate. Though its dynamics is determined by exterior factors such as velocity of the belt, stiffness springs, masses of the oscillators,

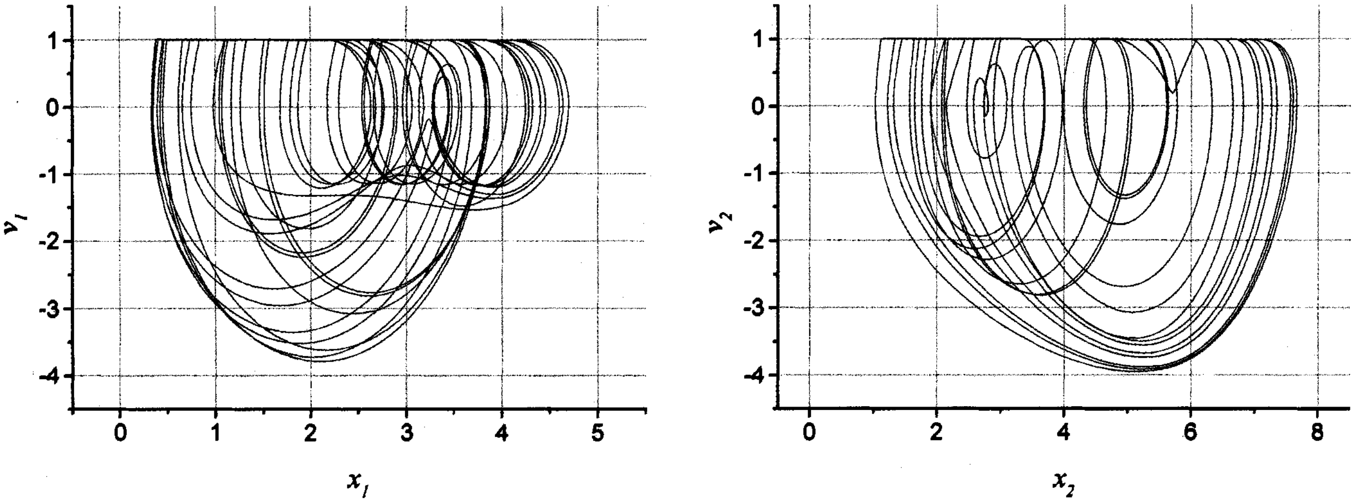

Fig. 11. Phase portraits of the trajectories of the first and second oscillators ($v_0 = 1$, $T_{01} = 30$, $T_{02} = 19.62$, $x_1(0) = 0.01$, $\dot{x}_1(0) = 0.5$, $x_2(0) = 0.01$, $\dot{x}_2(0) = 0.5$), which are corresponding to the domains of the chaotic vibrations in the (v_0, T_{01}) plane. Stick refers to the maximum "adhesion" time of the oscillators to the belt $2 < \max \Delta t_{\mathrm{st}\,1} < 5$, $5 < \max \Delta t_{\mathrm{st}\,2}$.

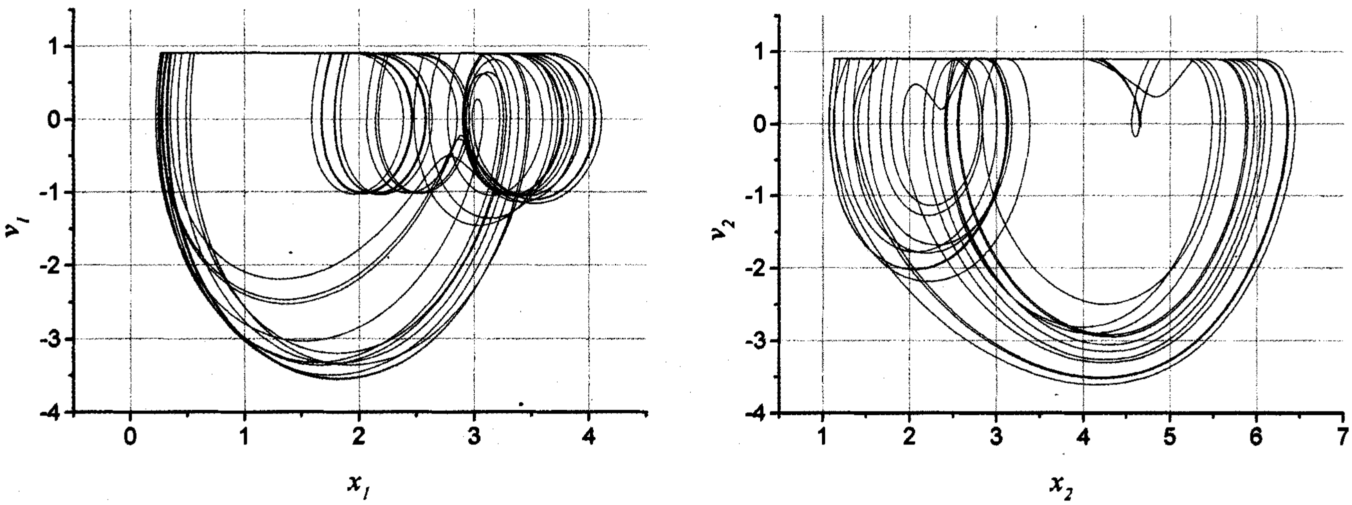

Fig. 12. Phase portraits of the trajectories of the first and second oscillators ($v_0 = 0.9$, $T_{01} = 29.43$, $T_{02} = 15$, $x_1(0) = 0.01$, $\dot{x}_1(0) = 0.5$, $x_2(0) = 0.01$, $\dot{x}_2(0) = 0.5$), which are corresponding to the domains of the chaotic vibrations in the (v_0, T_{02}) plane. Stick refers to the maximum "adhesion" time of the oscillators to the belt $2 < \max \Delta t_{\mathrm{st}\,1} < 5$, $5 < \max \Delta t_{\mathrm{st}\,2}$.

friction forces characteristic and initial conditions, questions emerge concerning the influence of oscillators on each other, to its interaction. For example,

- Does only one oscillator move chaotically or the chaotic motion of one of them involves the chaotic motion of other oscillator?
- Do the the oscillators move in different regimes: one oscillator moves with "adhesion" to the belt and the other one moves without "adhesion"?

Our investigations show that the situation when only one of the oscillators moves chaotically is not observed. However, there are conditions when only the first oscillator moves with "adhesion" to the belt and the other oscillator moves without "adhesion", and vice versa. It seems, that the motion without "adhesion" should be expected either for small values of the maximum static friction force (MSFF) or for comparatively large values of velocity of the belt. In considered conditions, critical values of the velocity of the belt v_{0i}^{cr} exist for i-oscillator ($i = 1, 2$) such that if $v_0 > v_{0i}^{\mathrm{cr}}$, then i-oscillator moves without "adhesion" to the belt for any values of MSFF. Thus, if we fix the MSFF of the second oscillator $T_{02} = 19,62$ (this

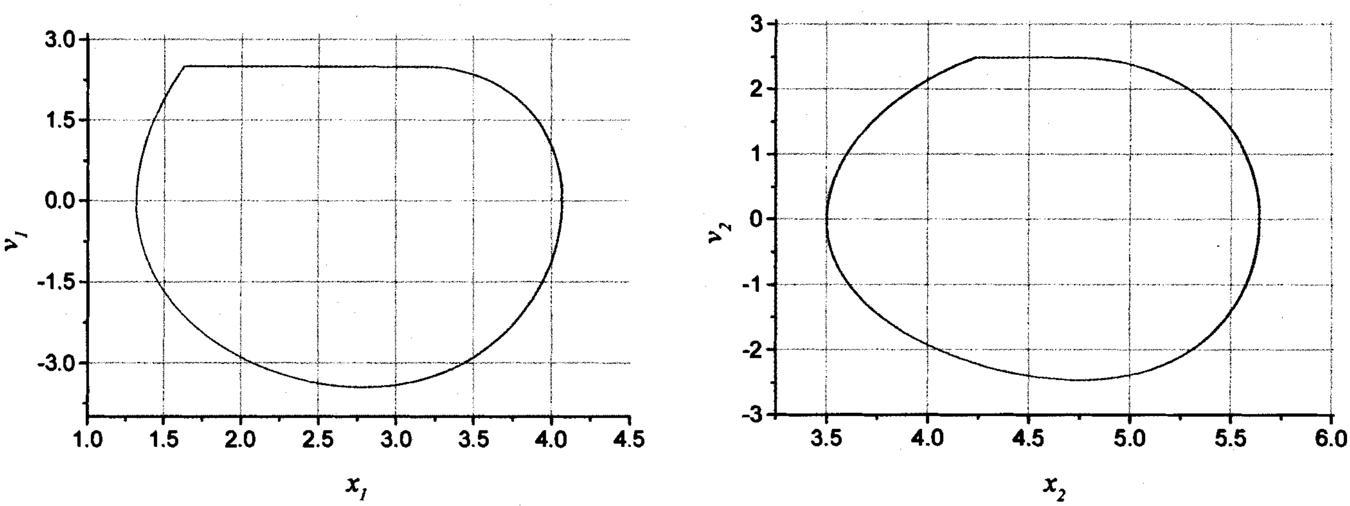

Fig. 13. Phase portraits of the trajectories of the first and second oscillators ($v_0 = 2.5$, $T_{01} = 30$, $T_{02} = 19.62$, $x_1(0) = 0.01$, $\dot{x}_1(0) = 0.5$, $x_2(0) = 0.01$, $\dot{x}_2(0) = 0.5$), which are corresponding to the domains of regular motion in the (v_0, T_{01}) plane. Stick refers to the maximum "adhesion" time of the oscillators to the belt $0.5 < \max \Delta t_{\mathrm{st}\,1} < 2$, $\max \Delta t_{\mathrm{st}\,2} < 0.5$.

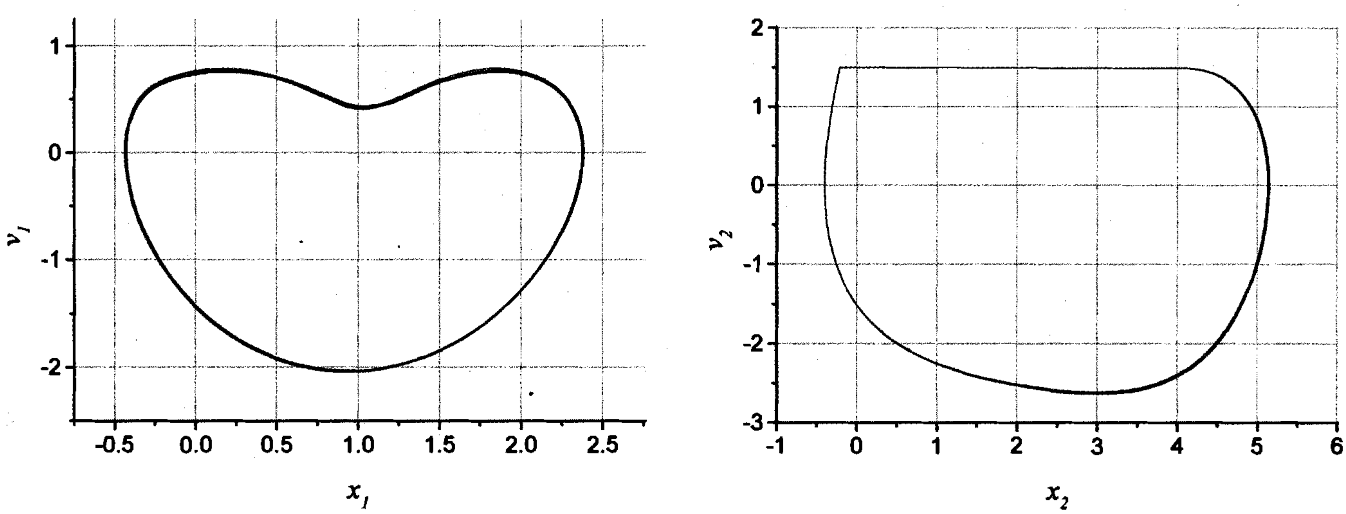

Fig. 14. Phase portraits of the trajectories of the first and second oscillators ($v_0 = 1.5$, $T_{01} = 0.5$, $T_{02} = 19.62$, $x_1(0) = 0.01$, $\dot{x}_1(0) = 0.5$, $x_2(0) = 0.01$, $\dot{x}_2(0) = 0.5$), which are corresponding to the domains of regular motion in the (v_0, T_{01}) plane. The first oscillator moves without stick. Stick of the second oscillator refers to the maximum "adhesion" time to the belt $2 < \max \Delta t_{\mathrm{st}\,2} < 5$.

value comparatively large), slip-slip regimes for the second oscillator are not observed when $v_0 < v_{02}^{\mathrm{cr}}$ (see Fig. 9). But for comparatively small values of the MSFF of first oscillator $T_{01} < 10$ the slip-slip motion of the first oscillator is observed in the neighborhood $1,5 < v_0 < 3$ (see Fig. 9). Similarly for sufficiently large value of the MSFF of the first oscillator $T_{01} = 29.43$ the slip-slip motion of the first oscillator is not observed when $v_0 < v_{01}^{\mathrm{cr}}$ (see Fig. 10). But for small values of the MSFF of the second oscillator $T_{02} < 5$ the second oscillator is in a slip-slip motion in the neighborhood $0,5 < v_0 < 2,5$.

Intending to find a slip-slip chaos, we compare Figs. 7 and 8 to 9 and 10 correspondingly. The small domain of chaotic vibrations is depicted in the neighborhood of $v_0 = 3,4$. Accordingly to Fig. 9 the stick-slip motion of the first oscillator and the slip-slip motion of the second oscillator are corresponding to this domain. As chaos is found in the neighborhood of $v_0 = 3,4$ and $v_{02}^{\mathrm{cr}} < 3.4 < v_{01}^{\mathrm{cr}}$, then only the second oscillator is in the slip-slip chaotic

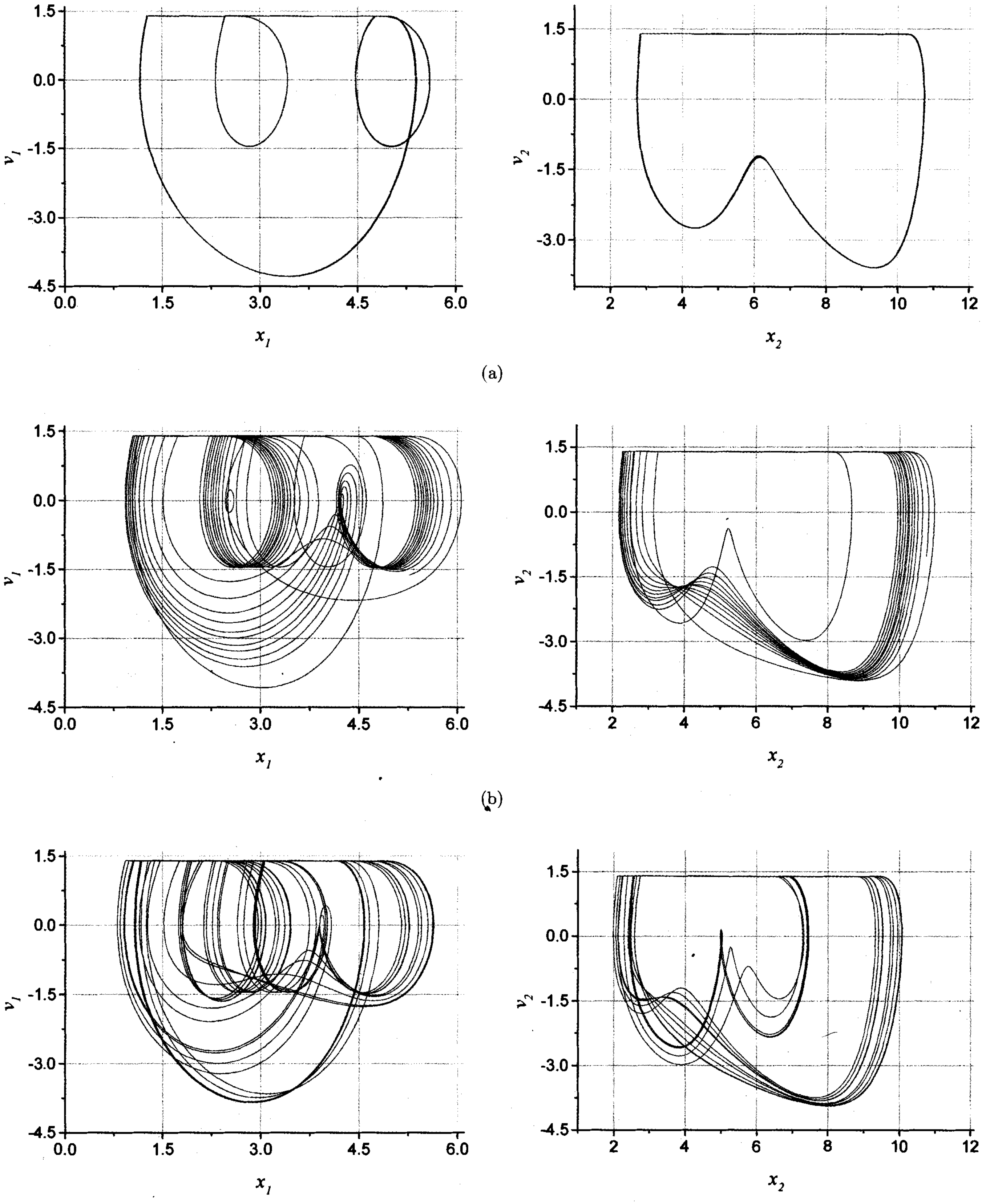

Fig. 15. Phase portraits of the trajectories demonstrating "chaos origin" with a passage from the stability domain (a) ($v_0 = 1.4$, $T_{01} = 29.43$, $T_{02} = 40$) to the instability domain. (b) ($v_0 = 1.4$, $T_{01} = 29.43$, $T_{02} = 34$), and (c) ($v_0 = 1.4$, $T_{01} = 29.43$, $T_{02} = 30$).

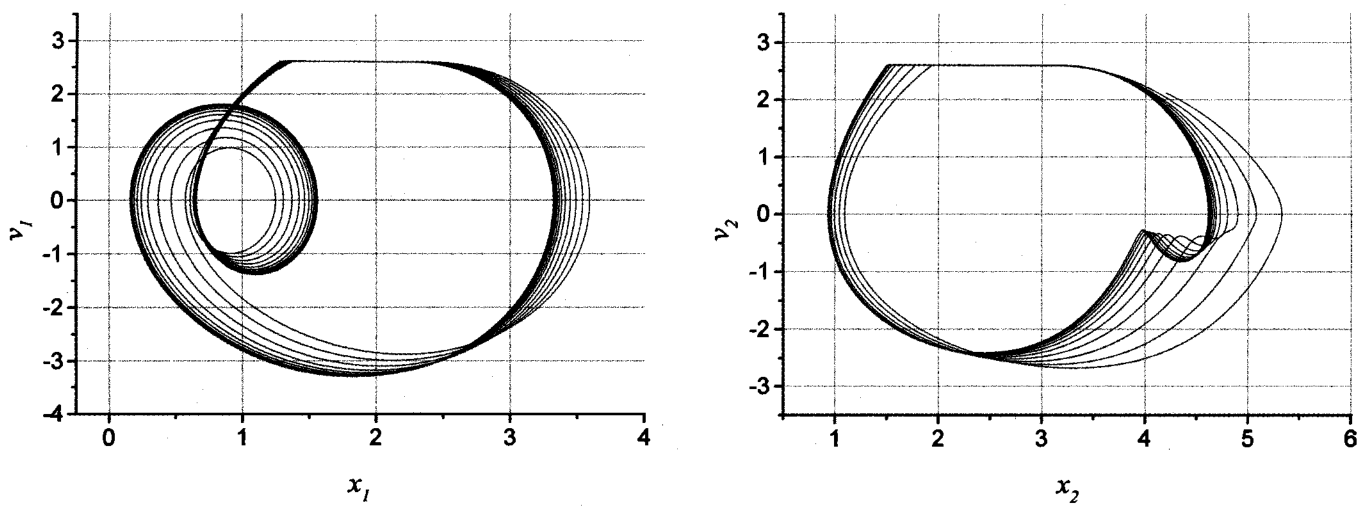

Fig. 16. Phase portraits of the trajectories of the first and second oscillators ($v_0 = 3.4$, $T_{01} = 41$, $T_{02} = 19.62$, $x_1(0) = 0.01$, $\dot{x}_1(0) = 0.5$, $x_2(0) = 0.01$, $\dot{x}_2(0) = 0.5$). The second oscillator is in slip-slip chaotic motion.

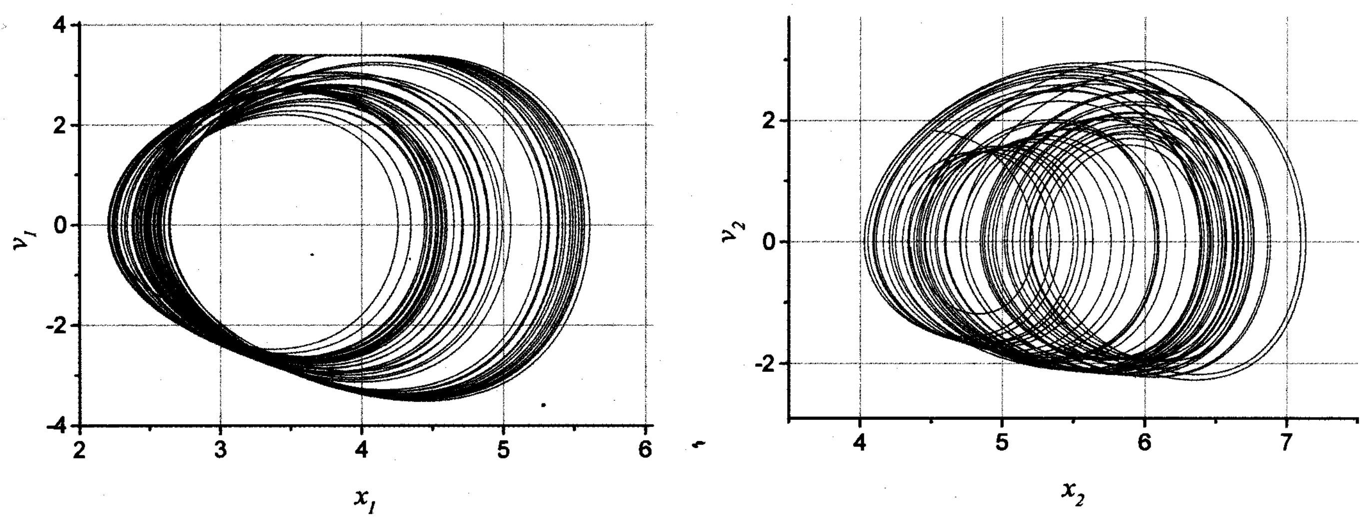

Fig. 17. Phase portraits of the trajectories of the first and second oscillators ($v_0 = 3.3$, $T_{01} = 29.43$, $T_{02} = 36$, $x_1(0) = 0.01$, $\dot{x}_1(0) = 0.5$, $x_2(0) = 0.01$, $\dot{x}_2(0) = 0.5$). The second oscillator is in slip-slip chaotic motion.

motion. Here, for considered conditions $v_{02}^{\mathrm{cr}} < v_{01}^{\mathrm{cr}}$. One can suppose that the largest domains of slip-slip motion of the oscillators are located in the parameter space (v_0, T_{01}, T_{02}) sections that correspond to more small values of the maximum static friction forces T_{01} and T_{02}. However, more detailed investigation (other parametric spaces, various sections of this spaces) exceeds the limits of the present work.

5. Conclusions

A direct and slightly modified application of the classical approach to quantify trajectories of a nonlinear system by choosing the observation of two close initial points of a phase space is outlined. The proposed method, in general, is much more simple and faster from a computational point of view than the well-known Wolf's algorithm.

The proposed method has been tested for different dynamical systems: the smooth one-degree-of-freedom Duffing oscillator, the Lorenz system and a nonsmooth self-excited two-degree-of-freedom mechanical system with friction. In the first case, a comparison with the results obtained via calculation of the Lyapunov exponents using Wolf's algorithm shows remarkable agreement. Also, in this case, domains of regular and chaotic motions in the parameter (Fig. 1) and initial conditions (Fig. 2) planes are reported.

In our second case, various regular and chaotic stick-slip and slip-slip dynamics are numerically traced and briefly discussed. Among others, it has been shown that for our investigated two-degrees-of-freedom system stick-slip chaos dominates, and slip-slip chaos is found to exist only for a narrow v_0 domain and for the second oscillator only.

References

Awrejcewicz, J., Kudra, G. & Lamarque, C.-H. [2002] "Nonlinear dynamics of triple pendulum with impacts," *J. Techn. Phys.* **43**, 97–112.

Awrejcewicz, J. & Olejnik, P. [2005] "Friction pair modeling by a 2-DOF system: Numerical and experimental investigations," *Int. J. Bifurcation and Chaos* **15**, 1931–1944 .

Brogliato, B. [1999] *Nonsmooth Impact Mechanics* (Springer-Verlag, London).

Holmes, P. J. [1979] "A nonlinear oscillator with a strange attractor," *Philos. Trans. R. Soc. London* **A292**, 419–448.

Kunze, M. [2000] *Non-Smooth Dynamical System*, Lecture Notes in Mathematics, Vol. 1744 (Springer-Verlag, Berlin).

Monteiro Marques, M. D. P. [1994] "An existence, uniqueness and regularity study of the dynamics of systems with one-dimensional friction," *Europ. J. Mech. A/Sol.* **13**, 277–306.

Moon, F. C. [1987] *Chaotic Vibrations* (Wiley, NY).

Oden, J. T. & Martins, J. C. A. [1985] "Models and computational methods for dynamics friction phenomena," *Comp. Met. App. Mech. Eng.* **52**, 527–634.

Oseledec, V. I. [1968] "A multiplicative ergodic theorem: Lyapunov characteristic numbers for dynamical systems," *Trans. Moscow Math. Soc.* **19**, 197–231.

Wolf, A., Jack, B., Swinney, H. L. & Vastano, J. A. [1985] "Determining Lyapunov exponents from a time series," *Physica* **D16**, 285–317.